The relationship between substrate roughness parameters and bond strength of ultra high-performance fiber concrete

Article *in* Journal of Adhesion Science and Technology · August 2013

DOI: 10.1080/01694243.2012.761543

CITATIONS
21

READS
321

4 authors:

Bassam Tayeh
Assistant Professor - Islamic University of Gaza
52 PUBLICATIONS **292** CITATIONS
SEE PROFILE

B.H. Abu Bakar
Universiti Sains Malaysia
76 PUBLICATIONS **590** CITATIONS
SEE PROFILE

Megat Azmi Megat Johari
Universiti Sains Malaysia
105 PUBLICATIONS **1,454** CITATIONS
SEE PROFILE

Mani Maran Ratnam
Universiti Sains Malaysia
108 PUBLICATIONS **834** CITATIONS
SEE PROFILE

Journal of Adhesion Science and Technology

Publication details, including instructions for authors and subscription information:
http://www.tandfonline.com/loi/tast20

The relationship between substrate roughness parameters and bond strength of ultra high-performance fiber concrete

Bassam A. Tayeh [a b], B.H. Abu Bakar [a], M.A. Megat Johari [a] & M.M. Ratnam [c]

[a] School of Civil Engineering, Universiti Sains Malaysia, Engineering Campus, Nibong Tebal, 14300, Pulau Pinang, Malaysia
[b] Engineering Division, Islamic University of Gaza, Gaza, Palestine
[c] School of Mechanical Engineering, Universiti Sains Malaysia, Engineering Campus, Nibong Tebal, 14300, Pulau Pinang, Malaysia

Version of record first published: 25 Feb 2013.

To cite this article: Bassam A. Tayeh , B.H. Abu Bakar , M.A. Megat Johari & M.M. Ratnam (2013): The relationship between substrate roughness parameters and bond strength of ultra high-performance fiber concrete, Journal of Adhesion Science and Technology, DOI:10.1080/01694243.2012.761543

To link to this article: http://dx.doi.org/10.1080/01694243.2012.761543

Journal of Adhesion Science and Technology, 2013
http://dx.doi.org/10.1080/01694243.2012.761543

Taylor & Francis
Taylor & Francis Group

The relationship between substrate roughness parameters and bond strength of ultra high-performance fiber concrete

Bassam A. Tayeh[a,b], B.H. Abu Bakar[a]*, M.A. Megat Johari[a] and M.M. Ratnam[c]

[a]*School of Civil Engineering, Universiti Sains Malaysia, Engineering Campus, Nibong Tebal 14300, Pulau Pinang, Malaysia;* [b]*Engineering Division, Islamic University of Gaza, Gaza, Palestine;* [c]*School of Mechanical Engineering, Universiti Sains Malaysia, Engineering Campus, Nibong Tebal 14300, Pulau Pinang, Malaysia*

(*Received 18 October 2012; final version received 3 December 2012; accepted 19 December 2012*)

The bonding that exists between the old concrete and the new concrete depends largely on the quality of substrate surface preparation. The accurate representation of substrate surface roughness can help determine very precisely the correct bonding behavior. In this work, an experimental investigation was carried out to quantify the normal concrete (NC) substrate roughness parameters and evaluate their relationship with the bonding performance of ultra high-performance fiber concrete (UHPFC), used as a repair material. The bond strength was quantified based on the results of the pull-off test, splitting cylinder tensile test, and the slant shear test. Three types of NC substrate surface preparation were used: as-cast (without surface preparation) as reference, wire-brushed, and sand-blasted (SB); the roughness of which was determined using an optical three-dimensional (3D) surface metrology device (Alicona Infinite Focus). It was observed from the result of the pull-off test that failure occurred in the substrate, even though adequate substrate surface roughness was provided. Moreover, analysis of the splitting cylinder tensile and slant shear test results showed that the substrate surface preparation method had a significant influence in bonding strength between UHPFC and the NC substrate. The composite UHPFC/NC substrate having a SB surface behaved closely as a monolithic structure under splitting and slant shear tests. An excellent correlation ($R^2 > 85\%$) was obtained between the substrate roughness parameters and the results of the splitting cylinder tensile and slant shear tests.

Keywords: roughness parameters; bond strength; UHPFC; repair material; substrate; pull-off test; splitting cylinder tensile test; slant shear test

1. Introduction

Repair and rehabilitation have recently drawn significant attention in the field of civil engineering. Although engineers have been repairing deteriorated structures for many years now, the rate of unsuccessful concrete repairs remains unacceptably high. Lack of knowledge on the influence of certain fundamental parameters is the reason achieving durable repairs is reduced to a 'hit-or-miss' procedure in certain circumstances.[1,2]

Repair systems are usually divided according to three different material phases: the repaired substrate phase, the repair material phase, and the interface phase between the substrate and repair material. Each phase plays a role in the durable repair of a system. Among the three phases, the interface phase is key to integrating repair systems.[3–5]

*Corresponding author. Email: cebad@eng.usm.my

The quality of the interfacial bond between a substrate and an overlay plays a complex role in the successful performance of a composite. Capturing optimal bond characteristics is of utmost importance. Optimal interfacial bond characteristics are case specific; in some instances, stress transfer is crucial. The crux of the matter is that by identifying requirements, one can engineer an optimal bond by implementing a reliable substrate surface roughening technique.[6,7]

A number of previous studies confirmed that the bond strength between two concrete layers is considerably influenced by the roughness of a surface substrate.[8–10] Surface roughness, when accurately measured, can lead to easy prediction of the bond behavior of externally applied composite.[11–13]

The improved durability and high compressive strength of ultra high-performance fiber concrete (UHPFC), in comparison with normal concrete (NC), suggest that this UHPFC is an attractive choice as a conventional overlay material. However, this solution can only be ensured by a strong mechanical bond between UHPFC as an overlay material and a substrate material.[14]

Increasing the efficiency of the interfacial transition zone between the new and old concrete in terms of bond strength and durability remains a challenge in concrete repair technology and is thus given considerable attention by researchers. This subject has been investigated numerous times, but only the bond strength is addressed in most cases. The quantification of substrate surface roughness should be studied to understand the bond mechanisms better. A number of studies have used UHPFC as a repair or composite material to strengthen NC structural members. However, very little information on the behavior of the bond between UHPFC as repair material and old concrete substrate is available.

This study presents and analyzes the results of an experimental study that aims to quantify old concrete substrate roughness parameters and their relationship with the bonding performance of UHPFC, which has been used as a repair material. An optical three-dimensional (3D) surface metrology device was used to evaluate the roughness parameters. A pull-off test, splitting cylinder tensile test, and a slant shear test were performed to assess mechanical bond strength in terms of direct tension, indirect tension, and shear. The correlations between the substrate roughness parameters and the bonding strength of the split cylinder tensile and slant shear tests are also discussed.

2. Roughness parameters

Several parameters were adopted to quantify the surface roughness and are presented in the following items according to ISO 4287 [15] by Equations (1)–(7). These parameters may be considered individually or combined.

2.1. Roughness amplitude parameters

R_a – The average roughness, as shown in Figure 1.

$$R_a = \frac{1}{l_m}\int_o^{l_m} |y(x)|\mathrm{d}x \tag{1}$$

where, l_m is the evaluation length; and $y(x)$ is the profile height at position x.

R_q – Root-Mean-Square Roughness: The root-mean-square average roughness of a surface is calculated from another integral of the roughness profile:

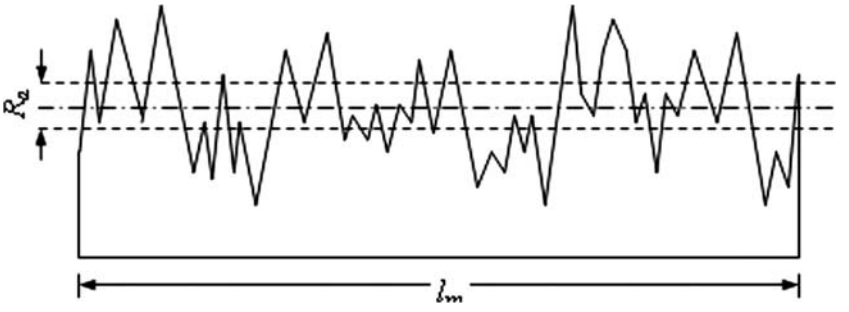

Figure 1. Average roughness, R_a.

$$R_q = \sqrt{\frac{1}{l_m}\int_0^{l_m} y^2(x)\mathrm{d}x} \tag{2}$$

R_t, R_p, and R_v: The peak roughness R_p is the height of the highest peak in the roughness profile over the evaluation length. Similarly, R_v is the depth of the deepest valley in the roughness profile over the evaluation length. The total roughness, R_t, is the sum of these two, or the vertical distance from the deepest valley to the highest peak.

$$R_p = |\max[y(x)]| \quad 0 < x < lm \tag{3}$$

$$R_v = |\min[y(x)]| \quad 0 < x < lm \tag{4}$$

$$R_t = R_p + R_v \tag{5}$$

R_z – The mean peak-to-valley height of roughness profile, as shown in Figure 2.

$$R_z = \frac{1}{5}\sum_{i=1}^{5} z_i \tag{6}$$

where, z_i is the peak-to-valley height in each cut-off length (λ_c).

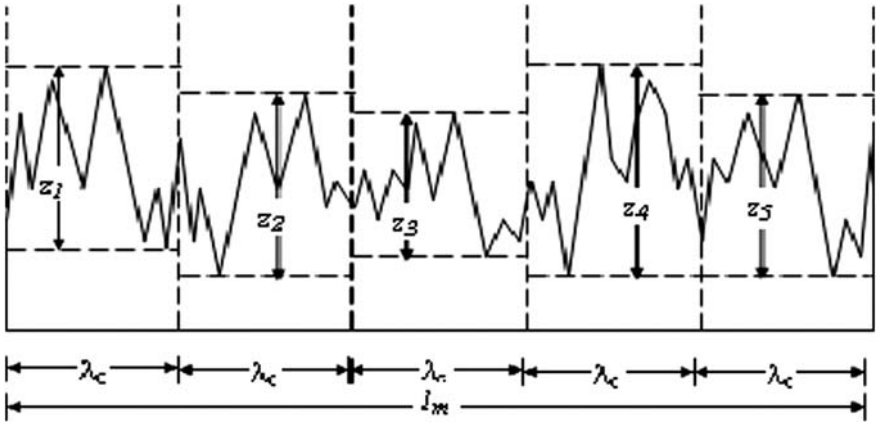

Figure 2. Mean peak-to-valley height, R_z.

2.2. Statistical parameters

R_q – Root-Mean-Square Roughness: The root-mean-square average roughness, R_q, was defined earlier. R_q is also a statistical parameter that measures the width of the amplitude distribution function (ADF): the wider the ADF, the larger the value of R_q, and the rougher the surface.

R_{sk} – Skewness: Skewness is another parameter that describes the shape of the ADF. Skewness is a simple measure of the asymmetry of the ADF, or, equivalently, it measures the symmetry of the variation of a profile about its mean line. Skewness is another parameter that describes the shape of the ADF.

$$R_{sk} = \frac{1}{l_m R_q^3} \int_o^{l_m} y^3(x)\mathrm{d}x \tag{7}$$

R_{sk} greater than about 1.5 in magnitude (positive or negative) indicates that the surface does not have a simple shape and a simple parameter such as R_a is probably not adequate to characterize the quality of the surface.

3. Experimental program

3.1. NC substrate and UHPFC properties

The NC used in this study was designed according to ACI 211 [16] guideline, using Type 1 Portland cement, natural river sand, crushed granite coarse aggregate, and a water/cement ratio of 0.5. Superplasticizer was used to achieve a slump value between 150 and 180 mm. The mix proportions are given in Table 1. At 28 days, tensile splitting and compressive strength tests were performed on cylindrical sample (100 mm diameter × 200 mm height) and prism sample (100 × 100 × 300 mm), respectively, as shown in Figure 3. The average strength values are 2.75 and 38 MPa for tensile splitting strength and compressive strength, respectively.

In the case of the UHPFC which was used as repair material, the mix proportions were adopted according,[17] using Type-I Portland cement, silica fume containing more than 92% silicon dioxide (SiO_2), mining sand, very high-strength straight steel micro-fiber (minimum tensile strength of 2500 MPa), and superplasticizer. The UHPFC registered an average flow value of 200 mm and 28 day's compressive strength in the average 170 MPa. The mix proportions for the UHPFC are given in Table 1.

Table 1. Mix proportions for NC substrate and UHPFC.

Concrete type (kg/m^3)	NC substrate	UHPFC
OPC (Type 1, 42.5R)	400	768
Coarse aggregate (max. 12.5 mm)	930	–
River sand (F.M. = 2.4)	873	–
Mining sand (<1180 μm)	–	1140
Silica fume (23.7 m^2/g)	–	192
Steel fiber (L_f = 10 mm, d_f = 0.2 mm)	–	157
Superplasticizer (PCE-based)	4	40
Water	200	144
Total	2407	2441
W/B	0.5	0.15
Cube strength, $f_{cc,28d}$	45 MPa	170 MPa
Splitting cylinder tension strength, $f_{sp,28d}$	3.18 MPa	15.3 MPa

Figure 3. Control specimens for (a) NC substrate, compression and (b) split cylinder tensile tests.

3.2. *Preparation of samples*

Each of the composite specimens comprised of NC as substrate and UHPFC as repair material. Samples representing the NC substrate were prepared using the proportions given in Table 1. After casting, the fresh samples were sealed and left to set in their respective molds for one day. On the next day, the specimens were removed from their molds, cleaned from dust and loose particles, and cured for two days in a water curing tank. Subsequently, the NC substrate specimens were taken out of the curing tanks. For surface roughening, three types of surface textures were used as shown in Figure 4: (i) as-cast (AC), i.e. without surface preparation as 'reference,' (ii) wire-brushed (WB) without exposing the aggregates, and (iii) sand-blasted (SB) to purposely expose the aggregates. As shown in Figure 5, an optical 3D surface metrology device (Alicona Infinite Focus), with 5X magnification and vertical resolution 1.6853 μm, was used to evaluate the degree of surface roughness. Figure 6 and 7(a) and (b) show NC substrate specimens of pull-off test, NC substrate halves of the splitting tensile test, and slant shear test samples with different surface textures, respectively. The roughened NC substrate specimens were then cured in water – which was maintained at room temperature up to 28 days from the casting date. After 28 days of curing, all the NC substrate specimens were taken out from the curing tank and left to dry for two months. Thus, the total duration applied to the NC substrate specimens before casting UHPFC as a repair material was three months.

Prior to casting the UHPFC, the surface of the roughened NC substrates was moistened for 10 min and dried with a damped cloth. The roughened and moistened NC substrates were then placed into their respective molds; in case of slant shear samples, the slanting side facing upward to be overlaid with the UHPFC. For the tensile splitting samples, the substrate halves with different surface textures were placed vertically at one side of the cylindrical molds, and the molds were then filled with UHPFC. The completed composite specimens for the pull-off, splitting tensile, and slant shear tests are shown in Figure 8(a), (b), and (c), respectively. The

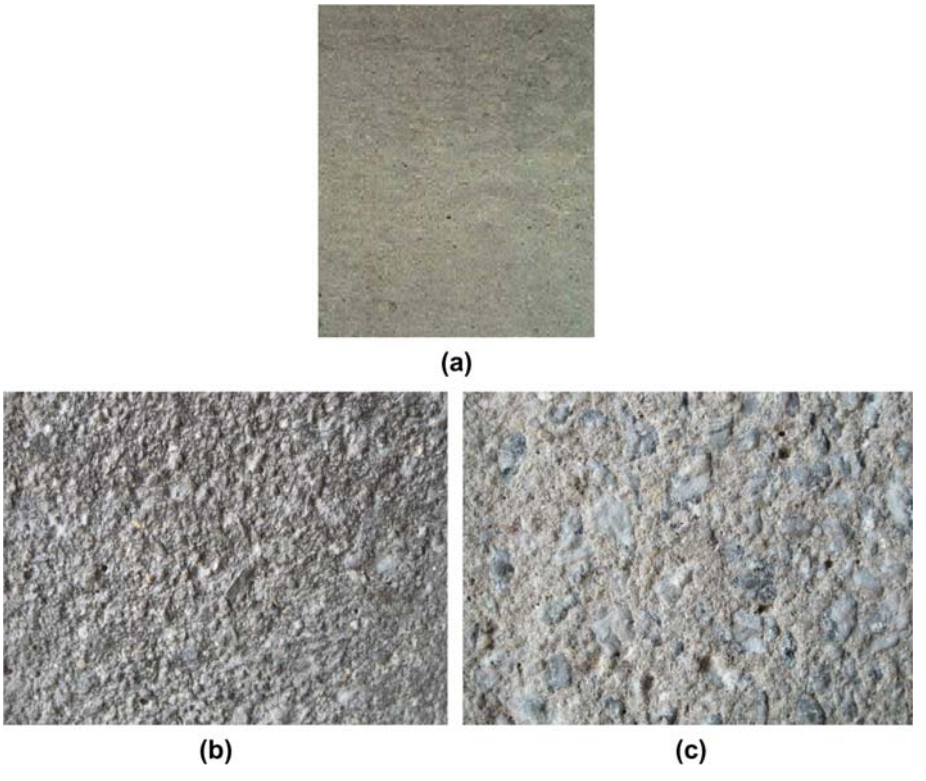

Figure 4. Substrate surface prepared with: (a) AC, (b) WB, and (c) SB.

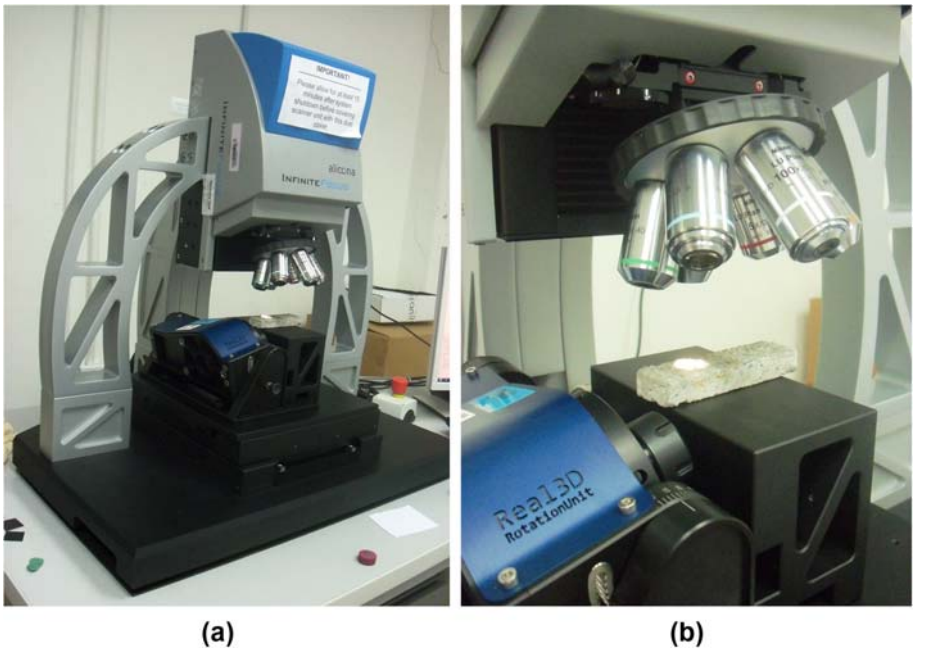

Figure 5. An optical 3D surface metrology device (Alicona Infinite Focus).

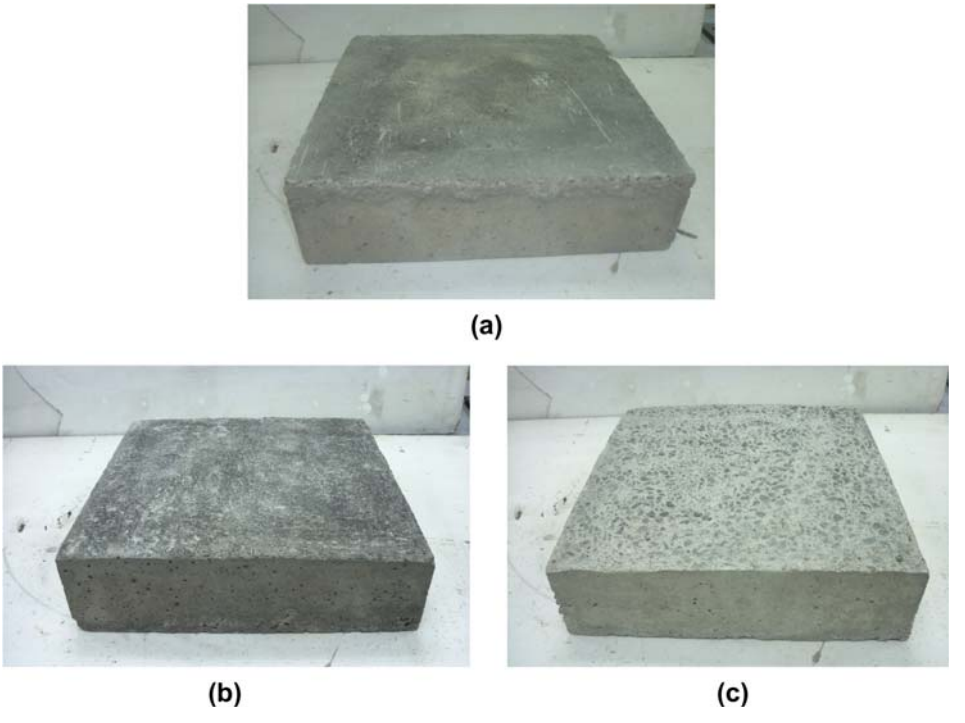

Figure 6. NC substrate with different surface textures (Pull-off test).

Figure 7. NC substrate halves samples with different surface textures: (a) split tensile test and (b) slant shear test.

composite specimens were then steam cured at 90 °C for 48 h.[18] The specimens were then cured in water – which was maintained at room temperature until the testing day. Pull-off test, splitting tensile test, and slant shear test were performed on third, seventh, and 28th days, respectively. One may argue on the practicality of the steam curing on actual *in situ* repair scenario, such as in the case of overlay. Nonetheless, this technique is very much feasible for *in situ* repair situations via the combination of heating mats, steam generators, and insulation systems, as being practiced in some precast and prestressed concrete industry sectors.[19–22]

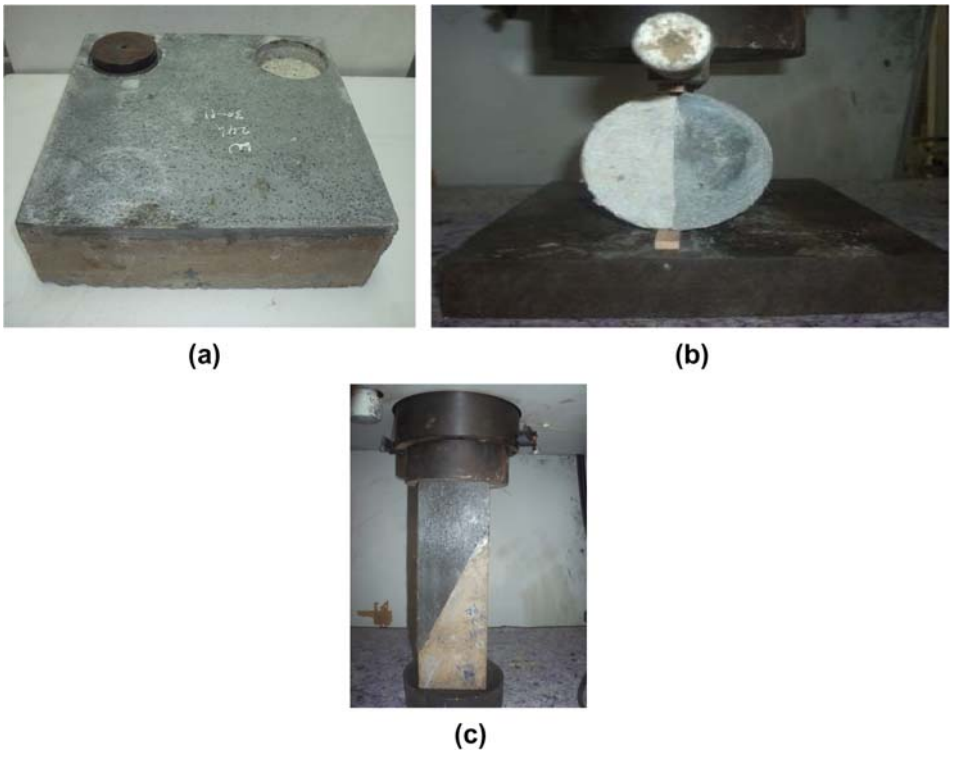

Figure 8. Setup of the composite UHPFC/NC substrate. (a) Pull-off test, (b) split tensile test, and (c) slant shear test.

3.3. *Pull-off test*

The pull-off test method is a common tensile test method used to assess the bond strength between the repair overlay and the existing concrete substrate. According to the ASTM D 4541 standard,[23] the pull-off test was chosen for two reasons: to evaluate the bond strength at the tension of the interface and it could be carried out *in situ*.[24]

The adopted geometry for the NC substrate specimens (300 mm × 300 mm × 80 mm thickness) was unreinforced concrete slabs. About 10 mm of UHPFC was cast as an overlay to the NC substrate. A core with a diameter of 75 mm was drilled into the composite specimens, and was further extended by 15 mm beyond the interface into the NC substrate. A circular steel disk was bonded with the core surface using epoxy glue. Tension force was applied to the disk. Figure 9 shows the schematic pull-off testing and specimen preparation.

The pull-off bond strength (S_{po}) was calculated by dividing the tensile (pull-off) force at failure (F_T) by the area of the fracture surface (A_f), as shown in Equation (8):

$$S_{po} = \frac{F_T}{A_f} \tag{8}$$

The pull-off test provides the most conservative bond measurement because it is not influenced by friction at the substrate surface.

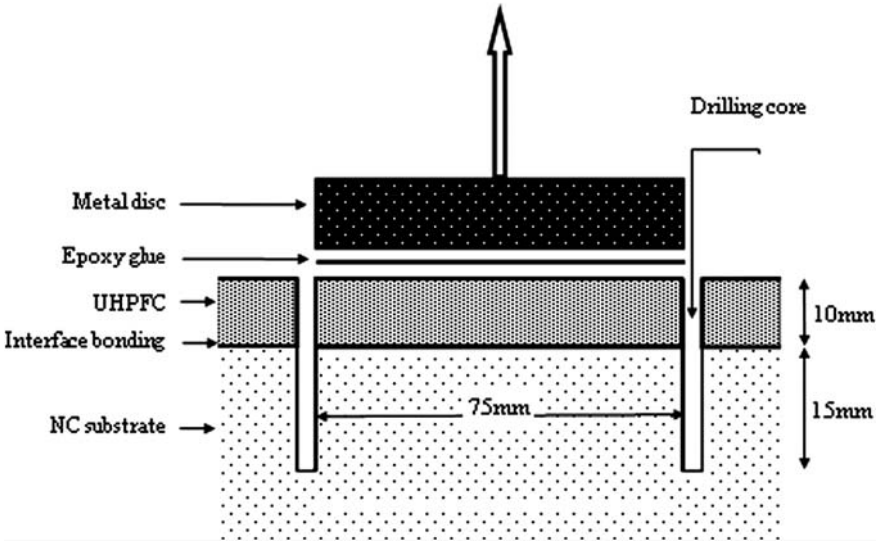

Figure 9. Schematic pull-off testing and specimen prepared.

3.4. *Splitting cylinder tensile test*

The splitting cylinder tensile test based on ASTM C496 [25] is an indirect tension test. The test is typically performed to determine the bond strength between the NC substrate and UHPFC. In the present experiment, UHPFC was cast and bonded to the NC substrate specimens to form a cylindrical composite cylinder (100 mm diameter × 200 mm height), as shown in Figure 5(a). The tensile strength of the splitting cylinder can be calculated using Equation (9) given by:

$$T = \frac{2P}{\pi A_T} \tag{9}$$

where, T is the tensile strength of the splitting cylinder (in MPa); P is the maximum applied load (in N); and A_T is the area of the bond plane (in mm^2). The bonded area can be taken as a nominal value of $200 \times 100 = 20{,}000\ mm^2$.

3.5. *Slant shear test*

The slant shear test method based on ASTM C882 [26] is a widely used test with a number of international codes.[27] This test was used in the current study to determine the bond strength between the NC substrate and UHPFC. Following this procedure, UHPFC was cast and bonded to the NC substrate specimens on a slant plane inclined vertically at a 30° to form composite prism specimens (100 mm × 100 mm × 300 mm), as shown in Figure 5(b). The bond strength for the slant shear was calculated by dividing the maximum measured load by the bonded area, which can be expressed as Equation (10):

$$\tau = \frac{P}{A_L} \tag{10}$$

where, τ is the bond strength (in MPa); P is the maximum recorded force (in N); and A_L is the area of the slant surface (in mm^2). The slant surface area can be taken as a nominal value of $100 \times 100/\sin 30° = 20{,}000\ mm^2$.

4. Results and discussion

4.1. Roughness parameters

Roughness parameters can be determined from the profile of surface roughness. In this study, the profiles of surface roughness for three types of surface textures of NC substrate specimens (AC surface, WB surface, and SB surface) were obtained using an optical 3D surface metrology device (Alicona Infinite Focus) as shown in Figure 10.

The parameters used to measure surface roughness are summarized in Table 2. It can be clearly inferred that, the type of substrate surface treatment adopted significantly impacts the values of roughness that were determined. The values of the roughness parameters obtained can be classified to be low, medium, and high for the AC surface, WB surface, and SB surface, respectively.

The values of roughness parameters obtained in this study are similar in range to those obtained by Garbacz et al. [28] and Santos et al. [29] They obtained a value of less than 1 mm for the peak-to-valley height of a SB substrate, wherein in the present study, the mean peak-to-valley heights was 0.122, 0.325, and 0.650 mm, and the maximum peak-to-valley heights was 0.214, 0.488, and 0.817 mm for the AC surface, WB surface, and SB surface, respectively.

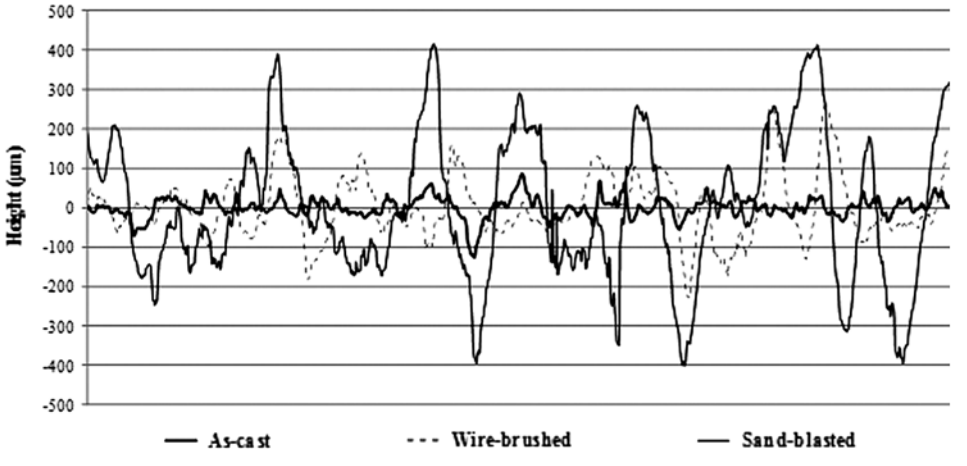

Figure 10. Roughness profile for different surface treatment: AC surface, WB surface, and SB surface.

Table 2. Roughness parameters.

Description	Name	Unit	AC	WB	SB
Average roughness of profile	R_a	µm	18.622	61.289	152.66
Root-Mean-Square roughness of profile	R_q	µm	25.795	80.673	184.85
Maximum peak-to-valley height of roughness profile	R_t	µm	214.3	488.52	817.36
Mean peak-to-valley height of roughness profile	R_z	µm	122.6	325.29	650.77
Maximum peak height of roughness profile	R_p	µm	86.477	259.49	415.41
Maximum valley height of roughness profile	R_v	µm	127.82	229.03	401.95
Mean height of profile irregularities of roughness profile	R_c	µm	88.626	273.29	578.75
Skewness of roughness profile	R_{sk}		0.799	0.525	0.170
Kurtosis of roughness profile	R_{ku}		6.7008	3.7475	2.425
Profile length	l_m	cm	4.00	4.00	4.00
Lambda C: cut off wavelength	λ_c	mm	8.00	8.00	8.00

Moreover, the values of the root-mean-square average roughness, R_q, was determined to be 0.0258, 0.0807, and 0.1848 mm for the AC surface, WB surface, and SB surface, respectively, according to ISO 4287 standard.[15] The higher the value of R_q, the rougher would be the surface texture.

In addition, the R_{sk} skewness value was estimated to be 0.799, 0.525, and 0.170 for the AC surface, WB surface, and SB surface, respectively, which was much less than 1.5, consequently, a simple parameter such as R_a is sufficient to adequately characterize the quality of the substrate surface.[15]

4.2. Pull-off test

The pull-off test results are shown in Table 3. Figure 11 shows that failure occurred in the NC substrate for all specimens and for all the different test ages. This is an indication of the existence of a strong bond with the UHPFC, regardless of the effect of substrate roughness. The bond that exists between the UHPFC and NC substrate was stronger than the tensile strength of the NC substrate. This increase in the pull-off strength could generally be attributed to greater adhesion and interlocking between the UHPFC and the substrate surfaces.[30] Therefore, it can be established from this result that UHPFC can eliminate the need for binder when used as overlay material.

Many previous works have observed zero value for pull-off test carried out to analyze the AC substrate surfaces.[29,31] However, in the present study, the bond strength obtained in the case of AC substrate surface was stronger than that for the NC substrate and was identical in strength to that of the SB surface. The bond strengths of the pull-off test obtained under test age of three days were 2.2, 2.33, and 2.26 MPa; 2.27, 2.23, and 2.22 MPa at a test age of

Table 3. Pull-off bond strength and failure mode.

		Test results at 3 days			Test results at 7 days			Test results at 28 days		
Surface treatment	Sample no.	F_T (kN)	S_{po} (MPa)	Failure mode	F_T (kN)	S_{po} (MPa)	Failure mode	F_T (kN)	S_{po} (MPa)	Failure mode
AC surface	AC1	9.6	2.17	Substrate	9.6	2.17	Substrate	9.1	2.06	Substrate
	AC2	9.1	2.06	Substrate	10.4	2.35	Substrate	9.9	2.24	Substrate
	AC3	10.5	2.38	Substrate	10.1	2.29	Substrate	11.5	2.60	Substrate
		Mean	2.20	Excellent	Mean	2.27	Excellent	Mean	2.30	Excellent
		COV	7.29		COV	4.03		COV	12.02	
Wire-brushed	WB1	11	2.49	Substrate	8.9	2.01	Substrate	10.3	2.33	Substrate
	WB2	9	2.04	Substrate	9.7	2.19	Substrate	11.1	2.51	Substrate
	WB3	10.9	2.47	Substrate	11	2.49	Substrate	9.4	2.13	Substrate
		Mean	2.33	Excellent	Mean	2.23	Excellent	Mean	2.32	Excellent
		COV	10.94		COV	10.74		COV	8.28	
SB	SB1	8.9	2.01	Substrate	9.2	2.08	Substrate	11.1	2.51	Substrate
	SB2	10.2	2.31	Substrate	9.8	2.22	Substrate	10.2	2.31	Substrate
	SB3	10.9	2.47	Substrate	10.4	2.35	Substrate	9.7	2.19	Substrate
		Mean	2.26	Excellent	Mean	2.22	Excellent	Mean	2.34	Excellent
		COV	10.15		COV	6.12		COV	6.87	

Note: Bond quality based on Table 4 [ACI concrete repair guide] [32] and Table 6 [33].

Figure 11. Failure of pull-off test through NC substrate. (a) Pull-off test setup and (b) failure of pull-off test.

seven days; and 2.3, 2.32, and 2.34 MPa at a test age of 28 days for the AC, WB, and SB surfaces, respectively.

The ACI concrete repair guide specifies a minimum acceptable bond strength range for direct tensile strength, as shown in Table 4. This guide is useful in the selection of appropriate repair materials.[32] In accordance with this guide and [33] (refer in Table 6), the characteristics of UHPFC having a bond strength more than 2.0 MPa easily surpass any other typical repair material. Thus, the UHPFC in all pull-off tests in this study can be categorized as 'excellent' because the bond strength is stronger than that of the NC substrate.

The excellent properties of UHPFC as a good repair material and binder for coupling with concrete substrate has been established from the pull-off tests carried out in this study, which demonstrated that the failure occurs only at the substrate. This significant increase in the bond strength can be attributed to the ability of silica fume, which is a key ingredient of UHPFC in improving the interfacial bond of the composite, both chemically and physically. The chemical reaction occurs between the active silicon dioxide (SiO_2) of silica fume in UHPFC and the $Ca(OH)_2$ in the NC substrate to form (C–S–H) gel. Furthermore, the silica fume in concrete refines the void system of cement paste, particularly the transition zone, thus making the transition zone to be more compact, dense, uniform, and strong.[34]

Table 4. Minimum acceptable bond strength range [ACI concrete repair guide] [32].

Description	Days	Bond strength (MPa)
Direct tensile bond	1	0.5–1.0
	7	1.0–1.7
	28	1.7–2.0
Slant shear bond	1	2.76–6.9
	7	6.9–12.41
	28	12.41–20.68

Table 5. Splitting tensile strength results and failure mode.

Surface treatment	Sample no.	Test results at 3 days			Test results at 7 days			Test results at 28 days		
		P (kN)	*T* (MPa)	Failure mode	*P* (kN)	*T* (MPa)	Failure mode	*P* (kN)	*T* (MPa)	Failure mode
AC surface	AC1	56.95	1.81	A	58.756	1.87	A	58.71	1.87	B
	AC2	48.714	1.55	A	61.28	1.95	B	52.70	1.68	A
	AC3	52.057	1.66	A	51.796	1.65	A	62.847	2.00	B
		Mean	1.67	Good	Mean	1.82	Very	Mean	1.85	Very
		COV	7.88		COV	8.57	good	COV	8.78	good
WB	WB1	70.60	2.25	C	62.5	1.99	B	99.543	3.17	C
	WB2	66.02	2.10	B	81.324	2.59	C	86.641	2.76	C
	WB3	82.251	2.62	C	76.029	2.42	C	92.428	2.94	C
		Mean	2.32	Excellent	Mean	2.33	Excellent	Mean	2.96	Excellent
		COV	11.47		COV	13.25		COV	6.96	
SB	SB1	105.28	3.35	C	103.88	3.31	C	121.25	3.86	C
	SB2	120.59	3.84	C	130.5	4.16	C	128.36	4.09	C
	SB3	108.49	3.46	C	98.371	3.13	C	107.58	3.43	C
		Mean	3.55	Excellent	Mean	3.53	Excellent	Mean	3.79	Excellent
		COV	7.25		COV	15.49		COV	8.87	

Note: Bond quality based on Table 6 [33].

Table 6. Quantitative bond quality in term of bond strength [33].

Bond quality	Bond strength, *T* (MPa)
Excellent	$\geqslant 2.1$
Very good	1.7–2.1
Good	1.4–1.7
Fair	0.7–1.4
Poor	0–0.7

4.3. Splitting test

The average values of the splitting cylinder tensile test results are shown in Table 5. The indirect tensile strengths of the different substrate surfaces were recorded in ascending order: AC surface, WB surface, and SB surface. The results show that different substrate surfaces were able to significantly enhance the indirect tensile strength of the composites when compared to the control (AC surface). At day 28 of the test, the relative percentage increase in tensile splitting was 58.7 and 103.3% for the WB surface and SB surface, respectively. This showed that sand-blasting was the most efficient surface preparation technique as it yielded the highest increase in the indirect tensile strength among the composites in comparison with the control.

Three types of failure modes of the splitting cylinder tensile test can be observed in Figure 12. These three failure types are represented as, Type A = pure interface failure, Type B = interface failure with partial substrate failure, and Type C = substratum failure. The results at all ages clearly show the relationship between the type of NC substrate surface treatment and bond strength and the failure mode in the splitting cylinder tensile test. The AC surface exhibited a combination of failure modes A and B, whereas the WB surface demonstrated a combination of failure modes B and C. In the case of SB surface, a Type C failure

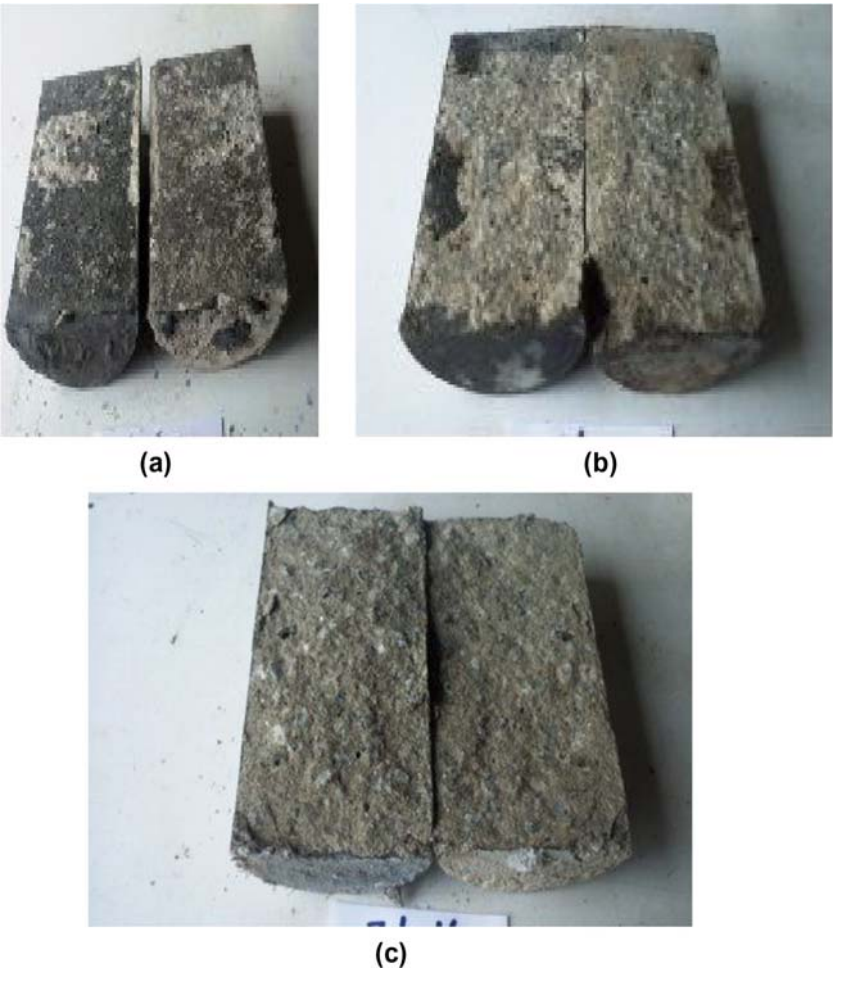

Figure 12. The failure modes of the splitting cylinder tensile test: (a) Type A failure, (b) Type B failure, and (c) Type C failure.

mode was observed, which indicates failure of NC substrate. This shows that SB surface has very high strength which can be attributed to the presence of more superior interfacial bond.

4.4. Slant shear test

Table 7 presents the average value of the bond strength in shear at different ages determined using the slant shear stress test. The overall test results showed that the types and characteristics of substrate surfaces significantly influence the shear bond strength.

In comparison to the control (AC surface), the recorded bond strength increased in the order of: AC surface < WB surface < SB surface. This shows that the treated substrate surfaces significantly improved the shear bond strength of the composites when compared to the control. This improvement, however, was characterized by a marked difference in the efficiency of the various types of substrate surfaces. The relative percentage increase in shear bond strength over the control at day 28 of the test was obtained to be 46.9% for the WB surface

Table 7. Slant shear strength results and failure mode.

Surface treatment	Sample no.	Test results at 3 days			Test results at 7 days			Test results at 28 days		
		P (kN)	τ (MPa)	Failure mode	P (kN)	τ (MPa)	Failure mode	P (kN)	S (MPa)	Failure mode
AC surface	AC1	193.6	9.68	B	144.1	7.21	A	147.63	7.38	A
	AC2	157.1	7.86	B	170.3	8.52	B	208.9	10.45	B
	AC3	140.27	7.01	A	193.7	9.69	B	164.39	8.22	B
		Mean	8.18	Good	Mean	8.47	Good	Mean	8.68	Poor
		COV	16.66		COV	14.65		COV	18.24	
WB	WB1	225.94	11.30	C	209.72	10.49	B	282.66	14.13	C
	WB2	246.38	12.32	C	263.34	13.17	C	213.31	10.67	B
	WB3	213.87	10.69	B	225.91	11.30	C	269.20	13.46	C
		Mean	11.44	Excellent	Mean	11.65	Very	Mean	12.75	Good
		COV	7.18		COV	11.81	good	COV	14.42	
SB	SB1	335.91	16.80	D	322.66	16.13	D	341.67	17.08	D
	SB2	351.13	17.56	D	370.06	18.50	D	362.94	18.15	D
	SB3↑	–	–	–	337.61	16.88	D	363.82	18.19	D
		Mean	17.18	Excellent	Mean	17.17	Excellent	Mean	17.81	Very
		COV	3.13		COV	7.06		COV	3.52	good

Note: ↑ Faulty specimen bond quality based on ACI concrete repair guide (see Table 4).

and 98.2% for the SB surface. Furthermore, all the treated substrate surfaces enhanced the shear bond strength at all test ages by 41.43 and 103.6% for the WB surface and SB surface, respectively. Thus, the SB surface exhibited the highest increase, making it the most efficient among all the studied composites.

The slant shear test specimens showed the following types of failure (Figure 13): Type A = interfacial failure or complete debonding at the transition zone; Type B = interfacial failure and substrate cracking or minor substrate damage; Type C = interfacial failure and substrate fracture; and Type D = complete substratum failure with sound interface. The results of the slant shear test indicated that the control (AC surface) exhibited Type A and B failure modes. Hence, the shear bond strength of the AC surface was the lowest among all the specimens because of the complete debonding failure brought about by the lack of surface preparation of the substrate. The observed trend emphasizes the need for appropriate surface preparation to ensure improved bond strength in composites. The WB surface exhibited a combination of Type B and C failure modes, whereas the SB surface exhibited Type D failure mode. The bond strength of the SB surface was the highest among all the treatment types according to the observed failure mode (complete substratum failure with no interfacial debonding). These findings concur with the similar trends obtained for splitting tensile strength carried out by previous researchers.[28,31,35] They demonstrated highest bond strength for SB surface while testing the effect of surface roughness between the concrete substrate and concrete repair.

The tremendous enhancement in the splitting tensile and slant shear bond strength can be attributed to greater adhesion and interlocking between the UHPFC and the roughened NC substrate surfaces. This is particularly true for the SB samples where the roughened or textured hardened NC matrix and the partially exposed aggregates promote superior adhesion along with excellent interlocking ability with the UHPFC. This ultimately contributes to the exceptional interfacial bond strength of the composite. In addition, silica fume plays a major

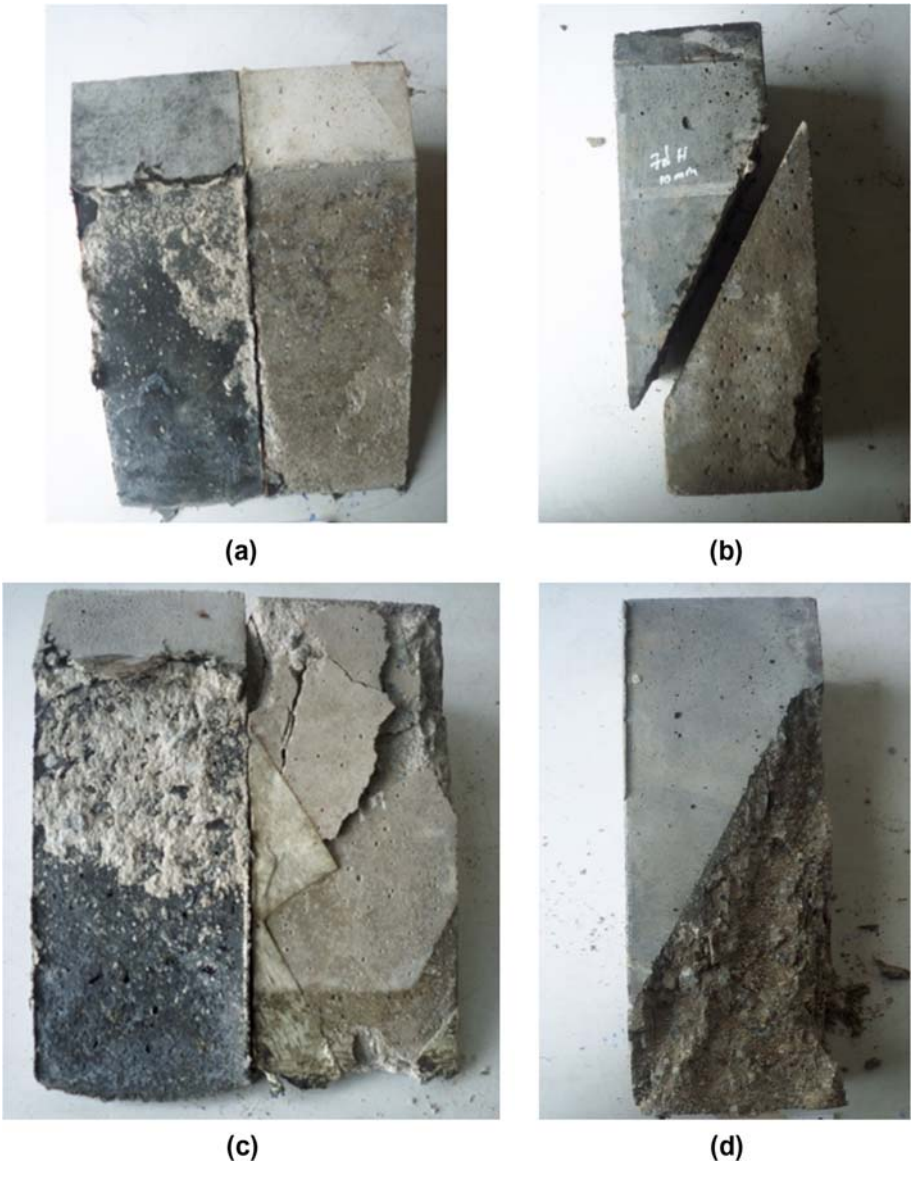

Figure 13. The failure modes of the slant shear test: (a) Type A failure, (b) Type B failure, (c) Type C failure, and (d) Type D failure.

role in enhancing the interface of the composite, both chemically and physically, hence establishing not only mechanical bond but possibly also chemical bond at the interface of the composite, a combination that could be termed as 'mechano-chemical' bond.[17]

4.5. Correlation between substrate roughness parameters and bond strength

A linear regression analysis was used to establish a model between the substrate roughness parameters and the bond strength. The substrate roughness parameter was considered as the

Table 8. Correlation between substrate roughness parameters and bond strength.

		Coefficient of correlation (R^2)					
		Splitting tensile strength			Slant shear strength		
Roughness parameters		3 days	7 days	28 days	3 days	7 days	28 days
Average roughness of profile	R_a	0.9453	0.8551	0.8652	0.9450	0.9197	0.8900
Root-Mean-Square roughness of profile	R_q	0.9462	0.8433	0.8797	0.9474	0.9218	0.8970
Maximum peak-to-valley height of roughness profile	R_t	0.9319	0.8194	0.9241	0.9350	0.9128	0.9088
Mean peak-to-valley height of roughness profile	R_z	0.9446	0.8378	0.8983	0.9470	0.9219	0.9043
Maximum peak-to-valley height of roughness profile within a sampling length	R_{max}	0.9302	0.8173	0.9258	0.9333	0.9114	0.9086
Maximum peak height of roughness profile	R_p	0.9068	0.7901	0.9381	0.9088	0.8914	0.9012
Maximum valley height of roughness profile	R_v	0.9456	0.8403	0.8916	0.9477	0.9223	0.9019
Mean height of profile irregularities of roughness profile	R_c	0.9451	0.8391	0.8951	0.9474	0.9221	0.9032

independent variable. As shown in Table 8, the substrate roughness parameters of the AC surface, WB surface, and SB surface presented good correlation with bond strength under indirect tension and in slant shear. All the tests demonstrated very high correlation ($R^2 > 85\%$) for all ages tested. Figures 14 and 15 show the correlation between the average roughness of profile (R_a) with splitting tensile strength and slant shear strength at different ages, respectively. These findings are in general agreement with the results of previous researchers,[28,31] who demonstrated that the splitting cylinder tensile test and slant shear test are sensitive to substrate surface treatment. The results of pull-off test show no correlation between the bond strength and the substrate surface roughness, since the failures occurred in NC substrate, regardless of substrate surface roughness employed. Thus, it can be inferred that the effect of chemical bond is stronger than the effect of the mechanical bond on the interfacial bonding. This is because the pull-off test is less sensitive to the substrate roughness.[36,37]

5. Summary and conclusions

The main findings of this study are summarized as follows:

(1) The results showed that to ensure efficient bonding between concrete substrate surfaces and overlay materials, the substrate surface preparation was necessary, since all the surface preparation methods experienced higher bond strengths when compared with that achieved by the AC (control) surface.

(2) The results of the splitting cylinder tensile test and slant shear test showed that the strength of bonding between UHPFC and the substrate was sensitive to substrate surface treatment, and depended on the method of substrate surface preparation. The average relative percentage increase in the splitting cylinder tensile test over the AC surface was 40.9 and 95.8% for the WB surface and SB surface, respectively. Furthermore, for the slant shear test, the average relative percentage increase over the AC surface was 41.43 and 103.6% for the WB surface and SB surface, respectively. The results of the pull-off test showed that the failure occurred in the substrates of all specimens at different test ages, even though the substrate surface was subjected to different roughness treatment.

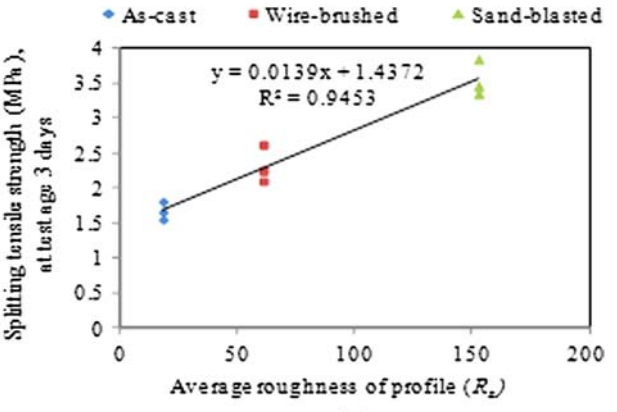

(a)

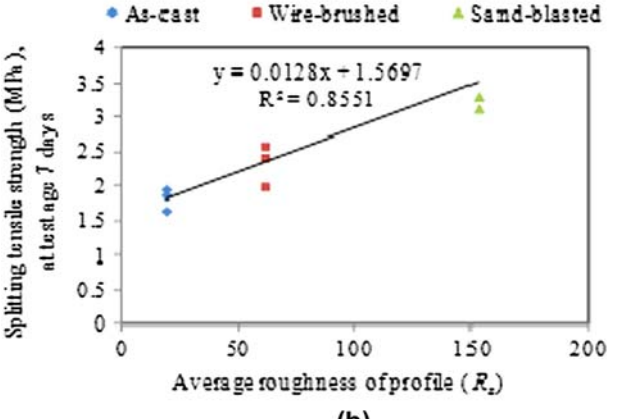

(b)

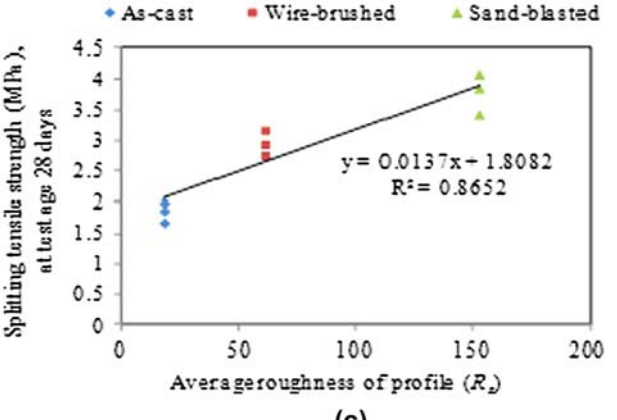

(c)

Figure 14. Correlation between average roughness of profile (R_a) and splitting tensile strength, at different ages: (a) Test age 3 days, (b) test age 7 days, and (c) test age 28 days.

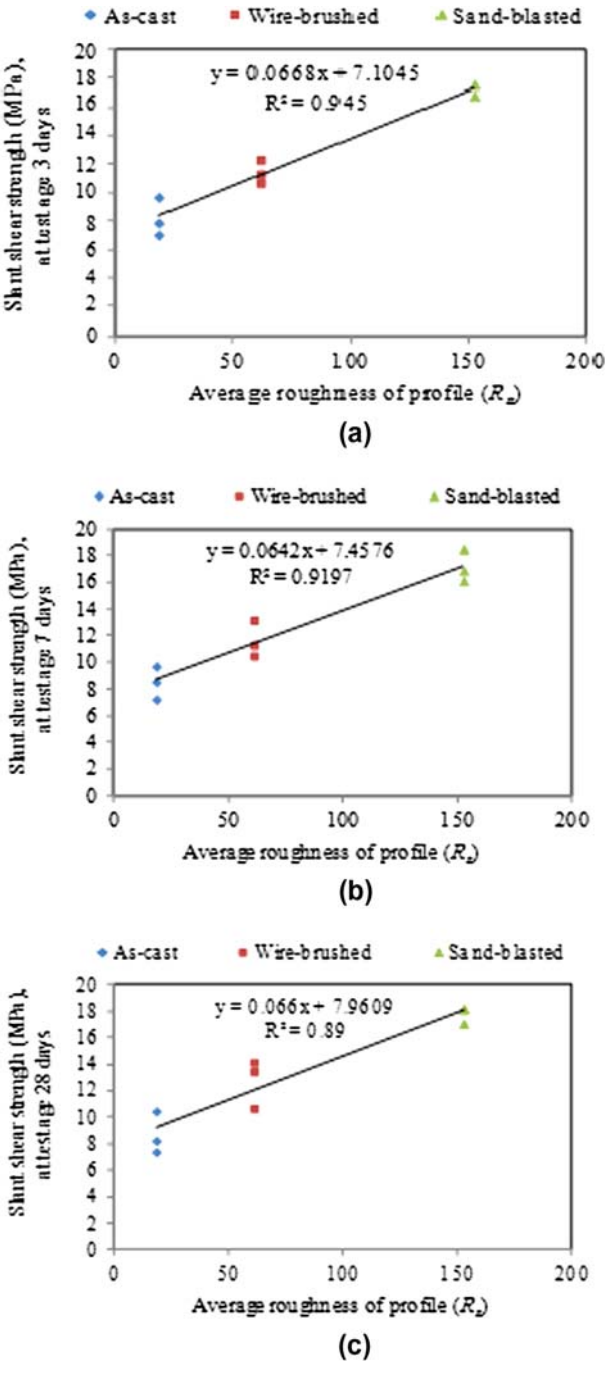

Figure 15. Correlation between average roughness of profile (R_a) and slant shear strength, at different ages: (a) Test age 3 days, (b) test age 7 days, and (c) test age 28 days.

(3) In this study, the SB method was demonstrated to be the most efficient technique because it yielded the highest increase in splitting tensile strength and shear bond

strength of the composite when compared with the control. In this case, the composite UHPFC/substrate behaved closely as a monolithic structure with higher substrate roughness parameter. Thus, it is established that UHPFC exhibits reliable and durable bonding performance for repaired and strengthened structural systems, and moreover, it ensures good resistance against the penetration of harmful substances.

(4) The linear regression analysis between the substrate roughness parameters and the bond strength proved that a very good correlation between the substrate roughness parameters and the splitting cylinder tensile test results and the slant shear test results was observed ($R^2 > 85\%$).

(5) Although no statistical evidence supports the relationship between bond behavior and the surface preparation technique for NC substrates and UHPFC overlays, all NC substrate surfaces should be SB prior to overlaying UHPFC as the repair material to ensure good bond strength.

Acknowledgment

The authors gratefully acknowledge Universiti Sains Malaysia for providing the financial support for this study.

References

[1] Perez F, Bissonnette B, Courard L. Combination of mechanical and optical profilometry techniques for concrete surface roughness characterisation. Mag. Concr. Res. 2009;61:389–400.
[2] Tayeh BA, Abu Bakar BH, Megat Johari MA, Voo YL. Utilization of ultra high performance fibre concrete (UHPFC) for rehabilitation – a review. The 2nd International Conference on Rehabilitation and Maintenance in Civil Engineering (ICRMCE-2); 2012 Mar 8–10; Solo, Indonesia.
[3] Vaysburd A, Emmons P. How to make today's repairs durable for tomorrow – corrosion protection in concrete repair. Constr. Build. Mater. 2000;14:189–197.
[4] Garbacz A, Courard L, Kostana K. Characterization of concrete surface roughness and its relation to adhesion in repair systems. Mater. Charact. 2006;56:281–289.
[5] Courard L, Michel F, Schwall D, Van der Wielen A, Garbacz A. Concrete substrate evaluation prior to repair. Mater. Charact. 2009;64:407–416.
[6] Diab H, Wu Z. Nonlinear constitutive model for time-dependent behavior of FRP-concrete interface. Contemp. Eng. Sci. 2007;67:2323–2333.
[7] Emmons PH, Vaysburd AM. Factors affecting the durability of concrete repair: the contractor's viewpoint. Constr. Build. Mater. 1994;8:5.
[8] Omar B, Fattoum K, Maissen B. Influence of the roughness and moisture of the substrate surface on the bond between old and new concrete. Contemp. Eng. Sci. 2010;3:139–147.
[9] Espeche AD, León J. Estimation of bond strength envelopes for old-to-new concrete interfaces based on a cylinder splitting test. Constr. Build. Mater. 2011;25:1222–1235.
[10] Duan K, Hu X, Mai YW. Substrate constraint and adhesive thickness effects on fracture toughness of adhesive joints. J. Adhes. Sci. Technol. 2004;18:39–53.
[11] Maerz NH, Chepur P, Myers JJ, Linz J. Concrete roughness characterization using laser profilometry for fiber-reinforced polymer sheet application. Transp. Res. Rec. J. Trans. Res. B. 2001;1775: 132–139.
[12] Destrebecq JF, Grédiac M, Sierra-Ruiz V. The transfer length in reinforced concrete structures strengthened with composite plates: experimental study and modelling. Compos. Sci. Technol. 2007;67:707–719.
[13] Perez F, Bissonnette B, Gagné R. Parameters affecting the debonding risk of bonded overlays used on reinforced concrete slab subjected to flexural loading. Mater. Struct. 2009;42:645–662.
[14] Tayeh BA, Abu Bakar BH, Megat Johari MA. Mechanical properties of old concrete – UHPFC interface. International Conference on Concrete Repair, Rehabilitation and Retrofitting III (ICCRRR 2012); 2012 Sep 2–5; Cape Town, South Africa.
[15] ISO BS. Geometrical product specifications (GPS) – surface texture: profile method – terms, definitions and surface texture parameters. 1997.

[16] ACI-211.1-91, Standard practice for selecting proportions for normal heavyweight, and mass concrete. ACI manual of concrete practice, part 1. American Concrete Institute; 1989.
[17] Tayeh BA, Abu Bakar BH, Megat Johari MA, Voo YL. Mechanical and permeability properties of the interface between normal concrete substrate and ultra high performance fiber concrete overlay. Constr. Build. Mater. 2012;36:538–548.
[18] Askar LK, Tayeh BA, Abu Bakar BH. Effect of different curing conditions on the mechanical properties of UHPFC. Awam International Conference on Civil Engineering (AICCE'12) and Geohazard Information Zonation (GIZ'12); 2012 Aug 28–30; Penang, Malaysia.
[19] Mangat P, Catley D. A novel low voltage heating system for curing and protection of early age concrete. Concr. Plant Int. 2005;4:106–112.
[20] Gerwick BC. Construction of prestressed concrete structures. New York (NY): John Wiley and Sons; 1993.
[21] Erdem T, Turanli L, Erdogan T. An important criterion to determine the length of the delay period before steam curing of concrete. Cem. Concr. Res. 2003;33:741–745.
[22] Tayeh BA, Abu Bakar BH, Megat Johari MA. Characterization of the interfacial bond between old concrete substrate and ultra high performance fiber concrete repair composite. Mater. Struct. 2012; doi 10.1617/s11527-012-9931-1.
[23] ASTM-C4541. Standard test method for pull-off strength of coatings using portable adhesion testers. West Conshohocken (PA): American Society for Testing and Materials; 1992. 19428–2959.
[24] Hindo KR. In-place bond testing and surface preparation of concrete. Concr. Int. 1990;12:46.
[25] ASTM-C496. Standard test method for splitting tensile strength of cylindrical concrete. West Conshohocken (PA): American Society for Testing and Materials; 1996. 19428–2959.
[26] ASTM-C882. Standard test method for bond strength of epoxy-resin systems used with concrete by slant shear. West Conshohocken (PA): American Society for Testing and Materials; 1999. 19428–2959.
[27] Naderi M. Analysis of the slant shear test. J. Adhes. Sci. Technol. 2009;23:229–245.
[28] Garbacz A, Gorka M, Courard L. Effect of concrete surface treatment on adhesion in repair systems. Mag. Concr. Res. 2005;57:49–60.
[29] Santos PMD, Julio ENBS, Silva VD. Correlation between concrete-to-concrete bond strength and the roughness of the substrate surface. Constr. Build. Mater. 2007;21:1688–1695.
[30] Lee MG, Wang YC, Chiu CT. A preliminary study of reactive powder concrete as a new repair material. Constr. Build. Mater. 2007;21:182–189.
[31] Julio ENBS, Branco FAB, Silva VD. Concrete-to-concrete bond strength. Influence of the roughness of the substrate surface. Constr. Build. Mater. 2004;18:675–681.
[32] Chynoweth G, Stankie RR, Allen WL, Anderson RR, Babcock WN. Concrete repair guide. ACI Committee, Concr. Repair Manual. 1996;546:287–327.
[33] Sprinkel MM, Ozyildirim C. Evaluation of high performance concrete overlays placed on route 60 over Lynnhaven inlet in Virginia. Charlottesville (VA): Virginia Transportation Research Council; 2000.
[34] Tayeh BA, Abu Bakar BH, Megat Johari MA, Zeyad AM. The role of silica fume in the adhesion of concrete restoration systems. Adv. Mater. Res. 2013;626:265–269.
[35] Van Zijl G, Stander H. SHCC repair overlays for RC: interfacial bond characterization and modelling. International Conference on Concrete Repair, Rehabilitation and Retrofitting II (ICCRRR 2009); 2009 Nov; Cape Town, South Africa.
[36] Tayeh BA, Abu Bakar BH, Megat Johari MA. Durability enhancement of the strengthened structural system joints. Hong Kong International Conference on Engineering and Applied Science (HKICEAS 2012); 2012 Dec 14–16; Hong Kong.
[37] Momayez A, Ehsani MR, Ramezanianpour AA, Rajaie H. Comparison of methods for evaluating bond strength between concrete substrate and repair materials. Cem. Concr. Res. 2005;35:748–757.